Uncertainty in Cloud Optical Depth Estimates Made from Satellite Radiance Measurements

ROBERT PINCUS

Geophysics Program, University of Washington, Seattle, Washington

MALGORZATA SZCZODRAK, JIUJING GU, AND PHILIP AUSTIN

Programme in Atmospheric Sciences, University of British Columbia, Vancouver, British Columbia, Canada

23 May 1994 and 2 December 1994

ABSTRACT

The uncertainty in optical depths retrieved from satellite measurements of visible wavelength radiance at the top of the atmosphere is quantified. Techniques are briefly reviewed for the estimation of optical depth from measurements of radiance, and it is noted that these estimates are always more uncertain at greater optical depths and larger solar zenith angles. The lack of radiometric calibration for visible wavelength imagers on operational satellites dominates the uncertainty retrievals of optical depth. This is true for both single-pixel retrievals and for statistics calculated from a population of individual retrievals. For individual estimates or small samples, sensor discretization (especially for the VAS instrument) can also be significant, but the sensitivity of the retrieval to the specification of the model atmosphere is less important. The relative uncertainty in calibration affects the accuracy with which optical depth distributions measured by different sensors may be quantitatively compared, while the absolute calibration uncertainty, acting through the nonlinear mapping of radiance to optical depth, limits the degree to which distributions measured by the same sensor may be distinguished.

1. Introduction

Operational weather satellites, though primarily intended to provide qualitative imagery for weather prediction, have become popular tools in atmospheric studies on large scales and in remote regions. Estimates of visible wavelength cloud optical depth from satellite measurements of visible wavelength reflectance have been made for more than a decade (Rossow et al. 1983; Arking and Childs 1985) and, with the advent of the International Satellite Cloud Climatology Project (ISCCP, Rossow and Schiffer 1991), are being produced routinely for the entire globe. Before such estimates can be used quantitatively (to determine temporal or spatial trends in optical depth or to validate the predictions of climate simulations, for example), a comprehensive understanding of the uncertainty in optical depth retrievals is required.

The uncertainty in cloud optical depth retrievals has been discussed by several authors in the context of cloud analysis algorithm development. Rossow et al. (1989) investigated the uncertainty introduced by computational factors, such as interpolation, and by various assumptions about the atmosphere and the clouds embedded in it made in the predecessor to the ISCCP algorithm. They reported uncertainties in single retrievals of cloud optical depth of 15%–20%, although they did not consider the dependance of the uncertainty on cloud optical depth or viewing and illumination geometry. King (1987) evaluated the sensitivity of optical depths estimated with an analytic asymptotic method to measurement errors, as well as imperfect knowledge of the single-scattering phase function and surface- and single-scattering albedos, and computed the numerical change in retrieved optical depth due to specified variations in the latter two parameters. Nakajima and King (1990) examined the impacts of instrument noise at the 5% level (or, equivalently, a 5% instrument calibration error) as a function of both optical depth and cloud droplet effective radius and found typical relative uncertainties in retrieved optical depth of as much as 50% at optical depths greater than about 50.

This note examines the uncertainty in cloud optical depths estimated from radiances observed by operational weather satellites. We consider uncertainties in retrieved optical depth introduced by imperfections in measurement techniques and in knowledge about the vertical structure of scattering and absorption in the atmosphere and explore how these errors affect individual estimates of optical depth, the uncertainty in

Corresponding author address: Robert Pincus, Climate and Radiation Branch, Code 913, NASA/GSFC, Greenbelt, MD 20771.

the statistical properties of population, and the degree to which two measurements can be accurately distinguished. We ignore, however, a fundamental problem that arises in the interpretation of radiance measurements in terms of cloud properties: the radiative transfer models upon which retrieval algorithms are based assume that each pixel is completely full of a uniform sheet of cloud so that the cloud optical depths retrieved strictly apply only to clouds that fit this description. Indeed, Rossow et al. (1989) point out that the largest uncertainty in the retrieval of *actual* (as opposed to *model*) cloud properties is the assumption of fully cloudy, homogeneous pixels. At this time, however, there exists no general way to evaluate the impact of non-plane-parallel geometry or internal variability in cloud optical properties on the retrieved optical depth. The uncertainty we discuss here, therefore, represents a lower bound on the true uncertainty.

In the next section we briefly review the theory underlying the retrieval of optical depth from satellite measurements of reflected solar radiation. Section 3 examines the role of measurement uncertainties (sensor discretization and calibration uncertainties) and model assumptions (the specification of column ozone abundance, cloud droplet size, and aerosol loading) on the uncertainty in the retrieval of cloud optical depth from a single radiance measurement. Section 4 considers how these errors are reflected in the statistical properties of large samples and in the difference between pairs of measurements, and section 5 offers some brief conclusions.

2. How optical depth is estimated from satellite radiance measurements

Remote sensing retrievals interpret top of the atmosphere radiance measurements in terms of cloud optical depth by comparing the *predictions* made by radiative transfer models of outgoing radiance as a function of cloud optical depth with *observations* of the radiance made by satellites. Here we briefly describe each step in the retrieval process with an eye to identifying sources of uncertainty in the final retrieval. We focus on the so-called look-up table methods; see King (1987) or Nakajima and King (1990) for a discussion of the asymptotic methods that have been applied to retrievals using radiance observations from high-altitude aircraft.

Initially, radiative transfer models are used to predict the pattern of outgoing radiance $L(\mu_0, \mu, \phi, \tau)$ at the top of the atmosphere—weighted by the solar spectrum and the spectral response of the observing instrument—as a function of cloud optical depth τ, solar zenith angle cosine μ_0, satellite viewing angle cosine μ, and the relative azimuth ϕ between the sun and the satellite. The effects of the surface underlying the cloud and the atmospheric column above the cloud are accounted for by constructing one or more model atmospheres in which the vertical distribution and total amount of scatterers (such as aerosols), absorbing gases (including water vapor and ozone), and surface albedo are specified. Model calculations are made at a variety of cloud optical depths and viewing and illumination angles, and the results are tabulated in look-up tables.

Satellite observations of outgoing radiance are discretized both in space, as pixels (picture elements), and in magnitude, as discrete brightness levels (instrument count values). To retrieve an optical depth from a satellite observation, the instrument count value at each pixel is reconverted to radiance L_{obs} through a calibration algorithm. Each pixel is assigned a latitude and longitude ("earth-located" or "navigated") from which the viewing and illumination geometry can be computed. After navigation and calibration, each pixel in the image is classified as clear or cloudy. [See Rossow et al. (1989) for a comprehensive review of many available techniques.] For each cloudy pixel the calculated radiance as a function of τ alone $L(\mu_0, \mu, \phi; \tau)$ is interpolated from the look-up table, and the optical depth for that pixel is chosen such that the observed reflectance matches the interpolated reflectance.

We have implemented a look-up table retrieval scheme based on numerical radiative transfer calculations made using the discrete ordinates method (Stamnes et al. 1988). We use the ISCCP satellite radiometer calibrations (Brest and Rossow 1992; Rossow et al. 1992; Desormeaux et al. 1993), which are available for a large number of sensors onboard geostationary and polar orbiting platforms from July 1983 to the present. The calibrations are normalized to the AVHRR sensor aboard *NOAA-7*, so our forward computations are made to predict the top of the atmosphere (TOA) radiance as observed by this instrument. In the discussions that follow, we use our implementation as an example, though the analysis could be applied to any similar algorithm. The details of the model computations and table look-up may be found in the appendix.

3. Uncertainty in individual estimates of cloud optical depth

In this section we compute the relative uncertainty introduced into a single optical depth retrieval by imperfect knowledge of both radiance at the satellite and the structure of the atmosphere. We do this by comparing the optical depth that would be retrieved by our algorithm if the actual radiance or atmospheric state differed from the nominal value reported by the satellite or assumed in the radiative transfer model. That is, we compute the relative uncertainty in optical depth

$$\frac{\Delta\tau_R(\mu_0, \mu, \phi, \tau)}{\tau_R(\mu_0, \mu, \phi, \tau)} = \frac{\tau_R(L'(\mu_0, \mu, \phi, \tau))}{\tau_R(L(\mu_0, \mu, \phi, \tau))} - 1, \quad (1)$$

where $L(\mu_0, \mu, \phi, \tau)$ is the TOA radiance calculated by our radiative transfer model using the nominal at-

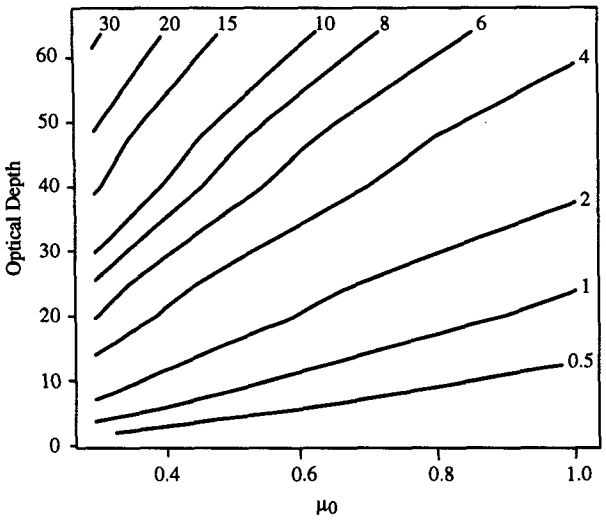

FIG. 1. Change in retrieved cloud optical depth in percent caused by a small constant change in TOA radiance L for the nominal atmosphere given in the first column of Table 1. The results have been averaged over all satellite zenith angles and relative azimuths. Uniform changes in reflectance correspond to larger changes in cloud optical depth as either solar zenith angle or cloud optical depth increases, implying that optical depth retrievals will be more uncertain as these quantities increase.

mospheric conditions and satellite calibrations described in the appendix, $L'(\mu_0, \mu, \phi, \tau)$ is a perturbation about the nominal state caused by changes in either the model atmosphere or in the radiance measured at the satellite, and $\tau_R(L(\mu_0, \mu, \phi, \tau))$ is the optical depth retrieved from the nominal lookup table.

a. *Uncertainty in optical depth retrievals increases with solar zenith angle and optical depth*

As other authors have demonstrated (see, for example, King and Harshvardhan 1986) the proportion of incident radiation reflected by a cloudy atmosphere increases with solar zenith angle, and this reflectance changes more rapidly with cloud optical depth as optical depth increases. Both phenomena affect the precision with which optical depth can be determined. This is evident in Fig. 1, which shows the change in retrieved cloud optical depth averaged over all values of μ and ϕ and introduced by a constant change in radiance [$\Delta\tau_R = \tau_R(L + \Delta L) - \tau_R(L)$, where L is the radiance look-up table predicted using the standard atmosphere, and ΔL is fixed at 1% of the instrument-response-weighted solar constant]. Note that a uniform change in TOA radiance corresponds to an increasingly large change in cloud optical depth as either optical depth or solar zenith angle increases. Since radiance is the quantity directly measured, and since all measurements have some degree of uncertainty associated with them, Fig. 1 has a well-known (e.g., King 1987; Nakajima and King 1990) but very important implication: *regardless of the skill with which radiance is measured at the top of the atmosphere, optical depth estimates are more uncertain at larger optical depths or larger solar zenith angles (smaller μ_0).* This sensitivity plays a prominent role in the results below.

b. *Measurement uncertainties*

1) DISCRETIZATION

Radiance values observed by a satellite radiometer at the top of the atmosphere are reported as discrete brightness levels or instrument counts by the data-processing stream so that each radiance reconstructed by a calibration algorithm is uncertain by an amount corresponding to ±0.5 count. The magnitude of this uncertainty can vary enormously between sensors. Figure 2 shows the relative uncertainty in TOA radiance (normalized by the instrument-weighted solar constant) due to discretization of radiances by the GOES VAS and AVHRR sensors. The VAS sensor encodes radiance as the square of the six-bit instrument count, while the AVHRR radiance is linear in the ten-bit count. (We have shown the sensitivity to eight-bit counts here, consistent with the ISCCP calibrations.) Figure 3 shows the uncertainty in retrieved optical depth introduced by the discretization, averaged over $\mu > 0.5$ and all ϕ, computed assuming that each radiance observed by the satellite is uncertain by ±0.5 instrument counts. Though the uncertainty in radiance depends only on instrument count value and decreases with nominal radiance, the uncertainty in retrieved optical depth shows the strong dependence on optical depth and solar zenith angle described above.

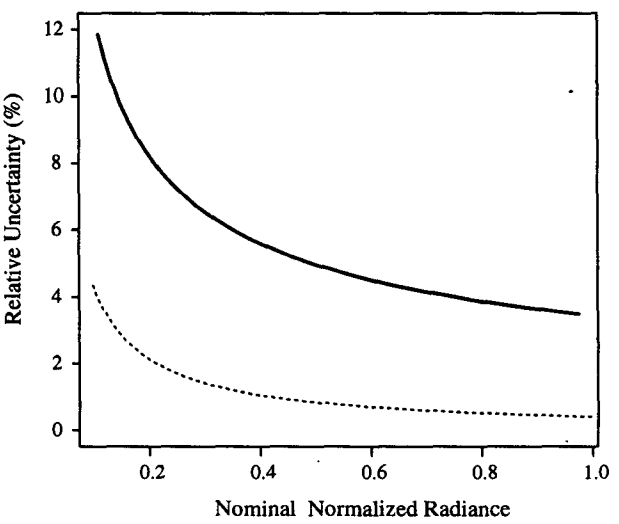

FIG. 2. Relative uncertainty (%) in TOA radiance (normalized by the instrument-weighted solar constant) due to discretization by the GOES VAS (solid line) and AVHRR (dashed line) sensors. Each radiance is uncertain by an amount corresponding to ±0.5 count.

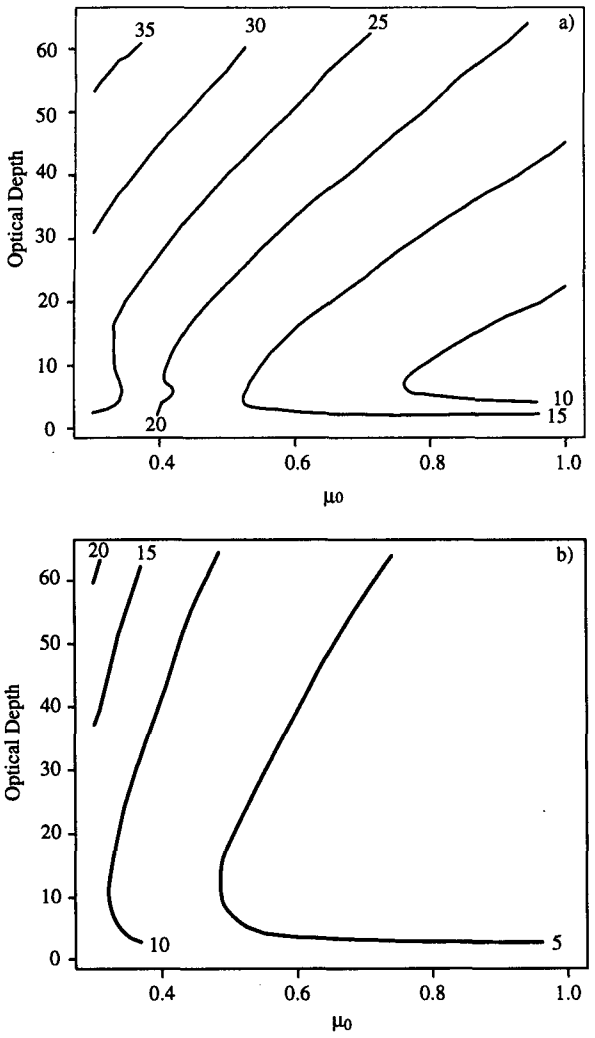

FIG. 3. Relative uncertainty (%) in retrieved optical depth $\Delta\tau_R/\tau_R$ due to discretization by (a) the six-bit quadratic GOES VAS sensor and (b) the eight-bit linear ISCCP AVHRR calibration. The results are averaged over all values of ϕ and over $\mu > 0.5$.

2) CALIBRATION

The current generation of visible band sensors aboard operational satellites are not calibrated in an absolute sense, so the conversion of instrument counts to radiance must be based on repeated observations of targets of known reflectance, or normalized to a standard sensor through comparison of observations from collocated, contemporaneous scenes. The ISCCP calibration algorithm combines the two approaches, normalizing the AVHRR sensor aboard each successive polar-orbiting satellite to the AVHRR aboard *NOAA-7*, then transferring the calibration to the other satellites in the program. There are two sources of uncertainty: the relative calibration between each pair of instruments in the program, which affects the degree to which measurements from different satellites or epochs may be compared, and the absolute (or radiometric) calibration, which affects the absolute magnitude of the retrieved values. The first uncertainty is estimated to be about 3% (Desormeaux et al. 1993); the second is estimated at between 5% and 10% (Han et al. 1994). Careful calibration for specific sensors (Kaufman and Holben 1993) or epochs (Whitlock et al. 1990) may reduce this calibration uncertainty at the expense of the ability to make comparisons with other times or places.

Figure 4 shows the relative uncertainty in retrieved optical depth due to calibration errors of 5% ($L' = 1.05 \times L$). Once again, although the calibration uncertainty is independent of both optical depth and solar zenith angle, the uncertainty introduced into the retrieval is an increasing function of both solar zenith angle and cloud optical depth. Nakajima and King (1990) reported a similar dependance of uncertainty on cloud optical depth (see their Fig. 9), although their use of spherical albedo rather than radiance masks the dependence of uncertainty on μ_0. Rossow et al. (1989) report uncertainties of 10%–20% in cloud optical depth due to an unspecified uncertainty in the absolute radiance calibration; we find that these values are exceeded for cloud optical depths greater than 20–25, depending on solar zenith angle.

An examination of long-term trends in the ISCCP dataset (Klein and Hartmann 1993) suggests that significant calibration errors may exist that are related to the intercalibration of the AVHRR instruments aboard the various polar orbiters. This effect is being assessed and will be reduced in the next version of the ISCCP data products. Recalibration will affect only the conversion of satellite counts to radiance, leaving the un-

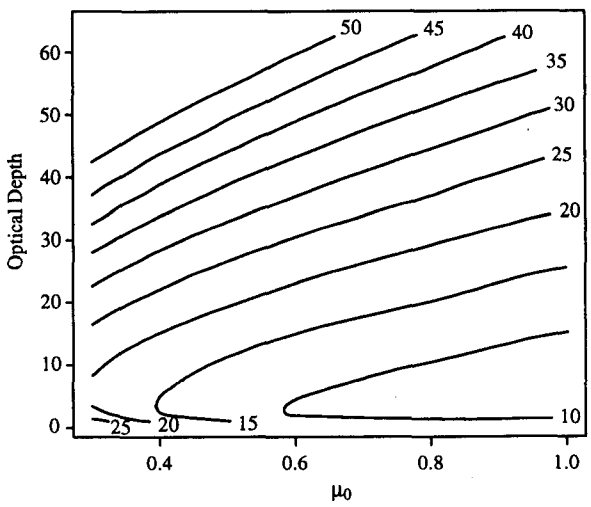

FIG. 4. Relative uncertainty (%) in optical depth introduced by a uniform 5% uncertainty in instrument calibration, averaged over all values of ϕ and over $\mu > 0.5$. Although the calibration uncertainty is constant, the uncertainty introduced in the retrieved optical depth values increases with solar zenith angle and with optical depth.

certainty as a function of cloud optical depth unchanged.

c. *Atmospheric model uncertainties*

The forward calculations of TOA radiance used in building the look-up tables require the definition of a standard or nominal model atmosphere in which we prescribe the vertical distribution and total amount of absorbing gases such as ozone and water vapor and scatterers such as aerosols and molecules (Rayleigh scattering). We must also choose a size distribution for the cloud drops (which is assumed to be independent of cloud optical depth) and reflectance characteristics for the underlying surface. For any particular observation, the value of any or all of these parameters may differ from the actual atmosphere. This lack of knowledge about atmospheric structure causes uncertainty in the predicted outgoing radiance, which in turn causes uncertainty in the retrieved optical depth.

We use the method of propagation of errors (Bevington and Robinson 1992) to evaluate the errors introduced into the retrieved optical depth by misspecification of the forward model. We treat the radiative transfer calculations as a general function:

$$L(\mu_0, \mu, \phi, \tau) = M(X_i), \tag{2}$$

where M is the model calculation and the X_i represent the input parameters to the model. If the model calculations change slowly with the input parameters, and changes in the parameters are small enough that they may be treated linearly, the variance in outgoing radiance due to the variance in a single-input parameter is

$$\mathrm{var}L = \mathrm{var}X\left(\frac{\partial M}{\partial X}\right)^2. \tag{3}$$

For independent changes in several model parameters, the total variance in radiance is

$$\mathrm{var}L = \sum_i \mathrm{var}X_i\left(\frac{\partial M}{\partial X_i}\right)^2. \tag{4}$$

We compile estimates of the observed variability of the radiatively active atmospheric constituents on seasonal timescales in Table 1. To assess the uncertainties introduced by misspecification of a constituent in our atmospheric model, we change the value of that constituent in the model atmosphere and recompute the look-up tables describing TOA radiance. We assume that the variability shown in Table 1 represents the standard deviation of each component, so that (3) reduces to

$$\mathrm{var}L = (L' - L)^2. \tag{5}$$

Figure 5 shows the relative error in TOA radiance $(\mathrm{var}L)^{1/2}/L$ caused by errors in aerosol amount, cloud drop effective radius, and ozone amount and the total relative error computed with (4). (We do not explore the impact of changes in the droplet single-scatter albedo since our Mie scattering calculations indicate its value is less than unity by only about 3×10^{-6}.) Figures 5a–c highlight the role each atmospheric component plays in modifying TOA radiance. The aerosol burden is mildly absorbing but has a higher backscattered fraction than do cloud droplets. Changes in aerosol loading change the outgoing radiance at the top of the atmosphere by a small amount, though the relative increase is significant only when the nominal radiance is small. Ozone is entirely absorbing, and its effects are proportional only to the pathlength through the atmosphere, which increases linearly with μ_0. Variations in the droplet size distribution affect outgoing radiance by changing the single-scattering phase function and the magnitude of the near-direct backscattering "hot spot" (see, for example, Fig. 9 of King 1987). The azimuthally averaged results shown are the result of changes in the relative proportions of forward and side scattering, though the uncertainty is largest near the hot spot.

Figure 6 shows the relative uncertainty in retrieved optical depth due to the sum of the uncertainties in all model parameters as computed using (1) and (4). Rossow et al. (1989) report that atmospheric effects on radiance (excluding variability in droplet size) introduce no more than a 5% error in optical depth, while variations in drop size from 5 to 20 μm introduce a 15% uncertainty in retrieved optical depth. The uncertainty shown in Fig. 6 falls between these estimates, largely because we consider a much narrower range of droplet size variability based on global observations of cloud droplet effective radius (Han et al. 1994).

d. *Total uncertainty*

Figure 7 shows the total uncertainty in individual retrievals of cloud optical depth introduced by sensor discretization and uncertainties in instrument calibration and model parameters (which we have assumed

TABLE 1. Nominal and perturbation radiative model parameters.

Quantity	Nominal value	Reference	Perturbation value	Reference
Column ozone amount	midlatitude summer	Kneizys et al. (1988)	nominal + 15%	Brasseur et al. (1985)
Drop effective radius	10 μm	Han et al. (1994)	12 μm	Han et al. (1994)
Aerosol optical depth	0.12	Kneizys et al. (1988)	0.20	Durkee et al. (1991)

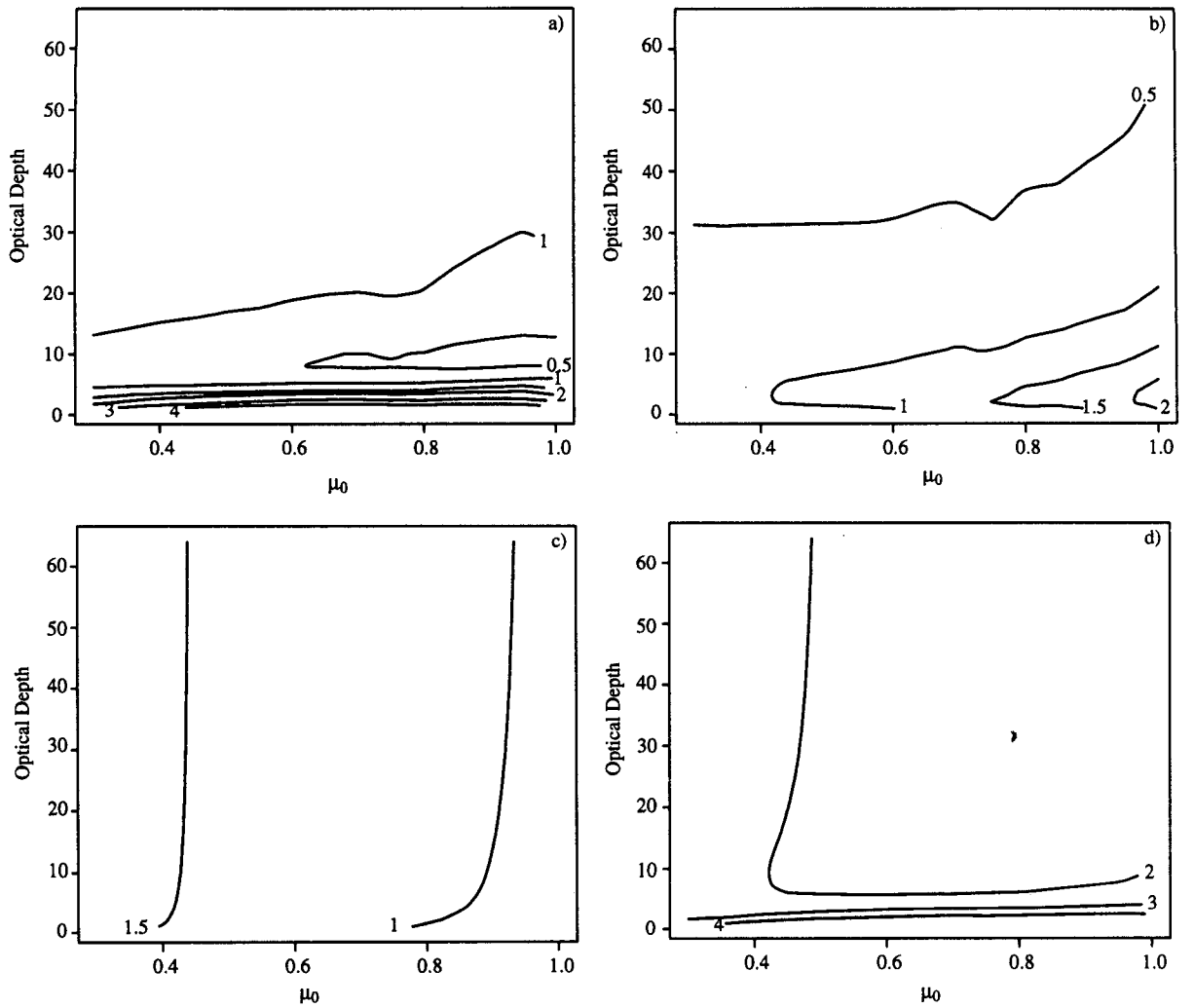

FIG. 5. Relative error (%) in computed TOA radiance $\Delta L/L$ introduced by perturbations in (a) aerosol optical depth, (b) cloud drop effective radius, and (c) ozone column abundance. Panel (d) shows the total relative error computed assuming that perturbations in the atmospheric constituents are uncorrelated. The changes are averaged over all azimuths and over satellite zenith angles < 60°. Standard and perturbation values for the atmospheric parameters are listed in Table 1.

are independent) for the VAS and AVHRR sensors. Uncertainty increases with increasing optical depth and increasing solar zenith angle since, as we have discussed, small changes in cloud reflectance correspond to large changes in optical depth in these regimes. For both sensors, the dominant source of uncertainty is the lack of radiometric calibration of the sensor; for the VAS sensor discretization outweighs the uncertainty due to misspecification of the forward model.

4. Applications: The uncertainty in derived quantities

The relative uncertainty in optical depth shown in Figure 7 is the uncertainty in a single estimate of cloud optical depth. One of the primary advantages of satellite remote sensing is its ability to determine cloud properties over large spatial domains and long timescales. In this section we consider the uncertainty in the mean optical depth of a sizable population of pixels and examine the uncertainty in the difference between the means of two populations obtained at different times or places.

a. Uncertainty in population means

With the exception of specialized studies [i.e., the susceptibility investigations of Platnick and Twomey (1994)], the statistical properties of a relatively large number of pixels are generally of greater interest than the value of a single observation. Uncertainty in statistical measures such as the mean value is affected by both systematic and random errors in the individual observations. The uncertainty due to random errors in

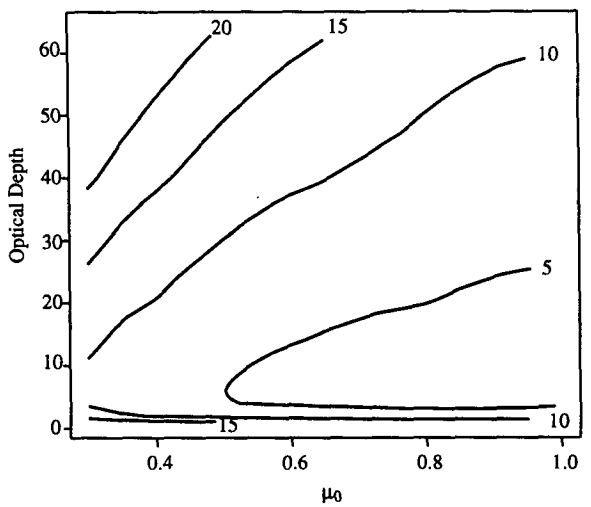

FIG. 6. Total relative change (%) in retrieved optical depth introduced by the uncertainty in TOA radiance shown in Fig. 5d.

the mean of a sample population of size N decreases as $N^{-1/2}$, while the absolute error in the mean due to systematic biases is the mean of the absolute uncertainties, irrespective of the number of observations. Random errors include those due to sensor discretization and local variations in atmospheric properties, while systematic errors arise from the uncertainty in absolute radiometer calibrations and consistent departures of the atmospheric conditions from those prescribed in the radiative transfer model.

To assess the uncertainty in the mean optical depth of a population of pixels, the random and systematic uncertainties associated with each pixel (which vary with cloud optical depth and viewing and illumination geometry) must be evaluated. As an example, we show in Fig. 8 histograms of TOA-scaled reflectance (radiance normalized by the instrument-weighted solar constant and the solar zenith angle) observed by GOES-West in a 1° region covered by marine stratocumulus clouds surrounding San Nicholas Island (33.3°N, 119.5°W) in the morning (0845 LST) and afternoon (1515 LST) of 14 July 1987 and the optical depths retrieved from those reflectances greater than the 0.15 threshold indicated. The mean optical depth in the morning (28) and afternoon (11) scenes shown here are large compared to the monthly average morning and afternoon optical depth values of about 15 and 5, respectively (Minnis et al. 1992).

What degree of uncertainty should be assigned to these mean values? The number of pixels in each images exceeds 10^4, so that errors due to discretization (which are of the same order of magnitude as calibration and model errors in individual observations) in each mean may be neglected. If we assume that the atmospheric model is correctly specified, the only remaining uncertainty in each mean value is that due to the absolute uncertainty in calibration, which leads to absolute error estimates of 5.9 and 1.2 (relative error of 21% and 11%) for the morning and afternoon means, respectively. If we include the total atmospheric model error (assuming that systematic but uncorrelated differences exist in all quantities between the model atmosphere and the atmosphere under observation), the absolute uncertainty in the morning and afternoon means increases slightly to 6.1 and 1.3 (relative errors 22% and 12%), respectively.

b. *Uncertainty in the difference between population means*

For some applications, including the computation of temporal trends, the uncertainty in the absolute value of cloud optical depth is less important than the

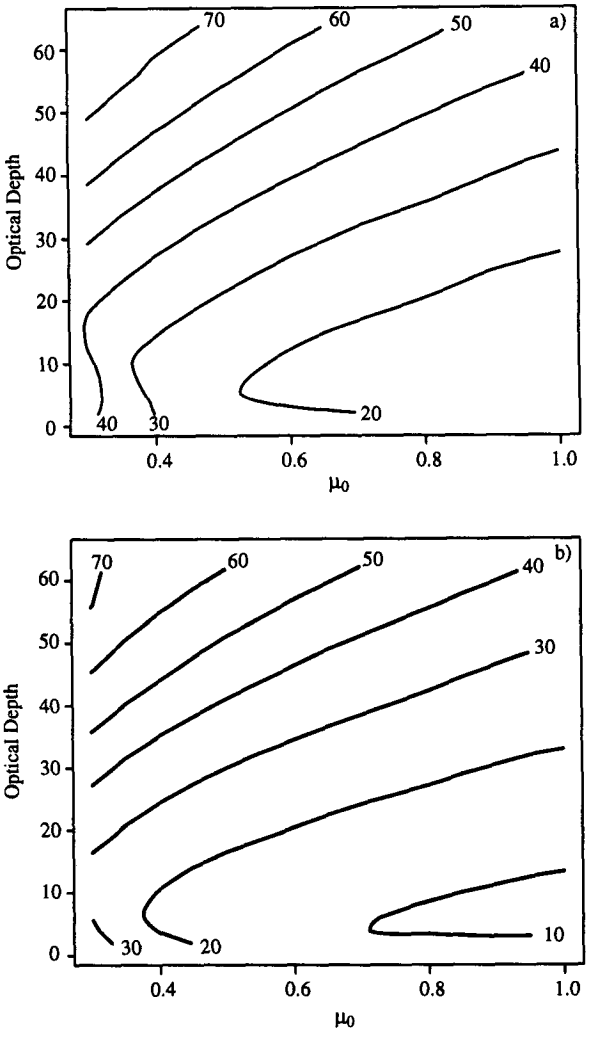

FIG. 7. Total relative uncertainty (%) in retrieved optical depth for (a) GOES VAS and (b) AVHRR sensors. Calibration uncertainties dominate both figures, while uncertainties in the model atmosphere are relatively unimportant.

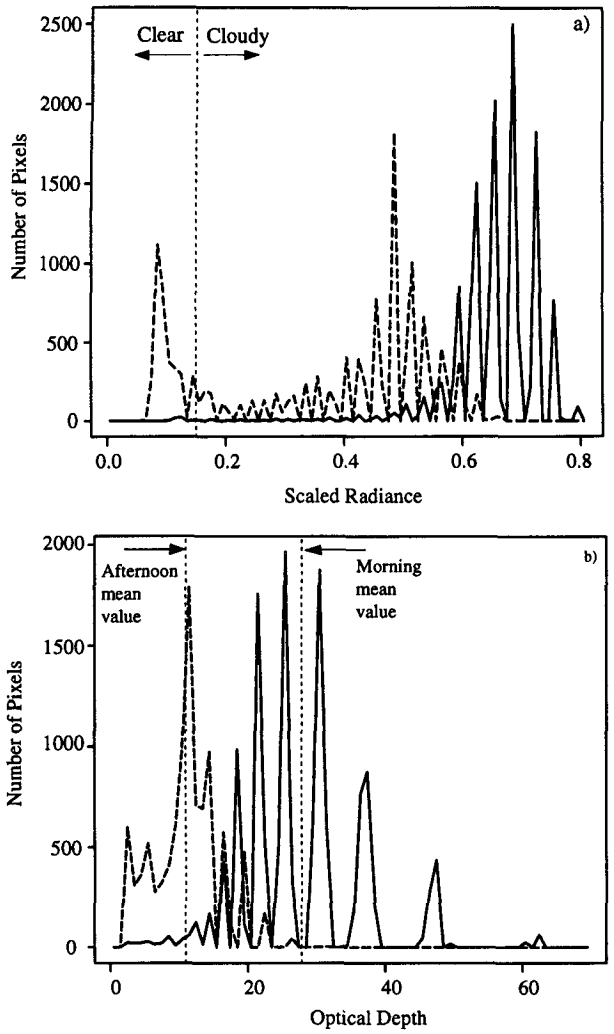

FIG. 8. Histograms of (a) scaled reflectance observed by GOES-West in a 1° region surrounding San Nicholas Island (33.3°N, 119.5°W) in the morning (0845 LST, solid line) and afternoon (1515 LST, dashed line) of 14 July 1987 and (b) the optical depths retrieved from radiances greater than the 0.15 threshold indicated by the dashed vertical line in (a). Reflectances and optical depths corresponding to individual instrument counts are clear, as is the sea surface albedo of about 8%. The means of the morning and afternoon optical depth distributions (28 and 11, respectively) are shown as dotted vertical lines in (b). Uncertainty in the absolute calibration of the satellite radiometer implies that the mean values are uncertain to about 22% and 12% for the morning and afternoon distributions, respectively. Furthermore, the nonlinear mapping of radiance to optical depth combines with the calibration uncertainty to cause an uncertainty in the difference between the morning and afternoon mean values of about 25%.

uncertainty in the difference between two temporally or spatially separated measurements. The relative uncertainty in sensor calibration affects the uncertainty in the difference if these measurements are made with different platforms or at substantially different times. The morning to afternoon difference in mean optical depth computed from the radiance distributions in Fig. 8, on the other hand, would appear to be very well constrained: both radiance distributions are measured by the same sensor, and local variations in ozone loading and aerosol optical depth are likely to be small over this short time interval. We might therefore expect that the uncertainty in the difference of the means is due only to the uncertainty in cloud droplet radius, which may change with time. Unfortunately, however, the nonlinear mapping of radiance to optical depth means that brighter (morning) pixels experience a larger change in optical depth than do darker pixels for a given absolute error in radiance calibration. Consider the radiance distributions shown in Fig. 8. Using the nominal radiometer calibration, the morning minus afternoon difference in cloud optical depth is 16.8. If each radiance is uniformly underestimated by 5%, we can compute a new difference in the means by increasing the value of each radiance and recomputing the optical depth distributions. Under these circumstances the difference in the mean increases to 21.7 (a 29% increase in the difference of the means). If we assume a radiance overestimate of the same magnitude, we find that the difference in the means is 13.3 (a 20% decrease).

The uncertainty in the difference of the means in this example represents an optimistic limit since the radiance distributions are measured using the same sensor (eliminating relative calibration uncertainties) at nearly the same times (which eliminates most random uncertainties in the atmospheric model even though the clouds are relatively thick). Nonetheless, the uncertainty in the difference of the means is substantial. Global studies such as ISCCP have the additional uncertainty introduced by the relative uncertainty in calibration between different sensors in the project, which is about 5%–10% for moderate optical depths and near-nadir solar zenith angles. Uncertainties in optical depth estimates (which are dominated by uncertainties in the calibration of satellite radiometers) imply that small relative changes in optical depth with time will be difficult to detect reliably.

5. Discussion

We have examined the uncertainty in optical depths retrieved from satellite measurements of reflected solar radiation. We find that regardless of the accuracy with which radiance is measured at the top of the atmosphere, optical depth retrievals are less precise at larger solar zenith angles and larger optical depths. We have shown that calibration uncertainties are the largest contributor to the uncertainty in the means of large samples. The calibration uncertainty also affects differences computed between samples (even those obtained with the same instrument) through the nonlinear mapping of radiance to optical depth. Since calibration uncertainties dominate the total uncertainty in retrieved optical depth, effort spent in refining the

atmospheric model for particular observations does not yield a large reduction in uncertainty. In other words, there is much more room for improvement in satellite sensor calibration than in radiative transfer modeling since these techniques are used in optical depth retrievals.

The uncertainty we compute in this note represents a lower bound on the true uncertainty in optical depth because we have assumed that the clouds for which the retrievals are being made are well represented by horizontally homogeneous, plane-parallel radiative transfer models. It is well known that both internal variability in cloud optical depth (see, for example, Cahalan et al. 1994) and the geometry of nonplane-parallel clouds (Kobayashi 1993) can affect the magnitude and angular distribution of the sunlight reflected from cloud layers. At present there exists no general method to quantitatively evaluate the impact of these effects on cloud optical depth retrievals, but this issue must clearly be addressed in the near future.

Acknowledgments. We appreciate helpful conversations with Steve Klein and Finbarr O'Sullivan, comments from Conway Leovy and Steve Warren, and the thorough reviews of two anonymous referees. We are grateful for support from NASA Graduate Fellowship in Global Change Research NGT-30047, Environment Canada Atmospheric Science Service, and the National Science and Engineering Research Council of Canada.

APPENDIX

Model Computations

We predict the TOA radiance observed by the *NOAA-7* AVHRR sensor using the discrete ordinates method (Stamnes et al. 1988). Our model atmosphere consists of three horizontally homogeneous, plane-parallel layers overlying an ocean surface. Cloud occupies the middle layer; the ocean beneath reflects isotropically with an albedo dependent on solar zenith angle (Minnis et al. 1992). All three layers contain radiatively active gases, aerosols, and molecules (Rayleigh scattering).

We calculate the single scattering parameters [single scattering albedo ω_0 and scattering phase function $P(\theta)$] of cloud droplets and aerosols at wavelength $\lambda = 0.65$ μm from Mie theory using the program of Wiscombe (1979, 1980). The cloud is represented as a lognormal distribution (Hansen and Travis 1974) of spherical drops of pure water with effective radius $r_{\text{eff}} = 10$ μm and variance $\nu = 0.05$; the aerosols follow a Haze-L number distribution (Diermendjian 1969). We use the refractive index of water from Hale and Querry (1973) and the empirical relationship for the refractive index of aerosols from Paltridge and Platt (1976), in which we assume a relative humidity of 70%.

We compute the cloud-free atmospheric transmittance of each layer in the model atmosphere using LOWTRAN-7 (Kneizys et al. 1988) in the wavelength range 0.50–0.80 μm, assuming a midlatitude summer atmospheric profile and the U.S. Navy standard marine aerosol model. LOWTRAN separately calculates the transmittance associated with each radiatively active gas, the aerosol, and the Rayleigh scattering in 5 cm^{-1} intervals. In this spectral region the only significantly absorbing gas is ozone (Saunders and Edwards 1989), so we average the LOWTRAN results into eight bands across which the ozone transmittance is smooth, then invert the atmospheric transmittance due to each atmospheric constituent to determine the absorption, aerosol, and Rayleigh-scattering optical depth in each layer and each band.

We determine the optical properties of each atmospheric layer in each spectral band by summing over the contributions from each atmospheric constituent (Tsay et al. 1989):

$$\tau = \sum_i \tau_i \tag{A1}$$

$$\omega_0 = \frac{\sum_i \omega_i \tau_i}{\tau} \tag{A2}$$

$$P(\Theta) = \frac{\sum_i \omega_i \tau_i P_i(\Theta)}{\sum_i \omega_i \tau_i}, \tag{A3}$$

where τ_i, ω_i, and P_i are optical depth, single-scattering albedo, and scattering phase function of the ith atmospheric constituent. We use the program of Stamnes et al. (1988) to determine the radiance at the top of the atmosphere in each band $L_j(\mu_0, \mu, \phi, \tau)$. We make computations at 48 values of ϕ, 24 values of μ, and 20 values of μ_0 evenly spaced in the ranges $\{0, 180°\}$, $\{0, 1\}$, and $\{0, 1\}$, respectively, and for $\tau = \{1, 2, 4, 6, 8, 10, 12, 14, 16, 18, 20, 24, 28, 32, 36, 40, 48, 56, 64, 80, 96, 112, 128\}$. Total TOA radiance L is calculated by summing over each spectral interval and by weighting the incident solar radiance and the instrument response.

To retrieve an optical depth from a satellite observation of radiance L_S, we use the location of the pixel and the time of day and day of year information to compute the viewing geometry (μ, ϕ) and solar zenith angle cosine (μ_0). We linearly interpolate along our look-up table to compute $L(\tau)$ for this set of angles, then use a root-finding algorithm (Press et al. 1986) to solve the equation $L_S - L(\tau) = 0$ by varying τ.

REFERENCES

Arking, A., and J. D. Childs, 1985: Retrieval of cloud cover parameters from multispectral satellite images. *J. Climate Appl. Meteor.*, **24**, 322–333.

Bevington, P. R., and D. K. Robinson, 1992: *Data Reduction and Error Analysis for the Physical Sciences.* second ed., McGraw-Hill, 328 pp.

Brasseur, G., A. J. Miller, P. K. Bhartia, A. Fleig, L. Froidevaux, H. Heath, E. Hilsenrath, J. A. Logan, P. McCormick, G. Megie,

R. Nagatani, J. M. Russel, and R. J. Thomas, 1985: Oxygen species. *Atmospheric Ozone 1985,* Vol II., World Meteorological Organization.

Brest, C. L., and W. B. Rossow, 1992: Radiometric calibration and monitoring of NOAA AVHRR data for ISCCP. *Int. J. Remote Sens.,* **13,** 235–273.

Cahalan, R. F., W. Ridgway, W. J. Wiscombe, T. L. Bell, and J. B. Snider, 1994: The albedo of fractal stratocumulus clouds. *J. Atmos. Sci.,* **51,** 2434–2455.

Desormeaux, Y., W. B. Rossow, C. L. Brest, and C. G. Garrett, 1993: Normalization and calibration of geostationary satellite radiances for the International Satellite Cloud Climatology Project. *J. Atmos. Oceanic Technol.,* **10,** 304–325.

Diermendjian, D., 1969: *Electromagnetic Scattering on Spherical Polydispersions.* American Elsevier, 290 pp.

Durkee, P. A., F. Pfeil, A. Frost, and R. Shema, 1991: Global analysis of aerosol particle characteristics. *Atmos. Environ.,* **25A,** 2457–2471.

Hale, G. M., and M. R. Querry, 1973: Optical constants of water in the 200-nm to 200-μm wavelength region. *Appl. Opt.,* **12,** 555–563.

Han, Q., W. B. Rossow, and A. A. Lacis, 1994: Near-global survey of effective droplet radii in liquid water clouds using ISCCP data. *J. Climate,* **7,** 465–497.

Hansen, J. E., and L. D. Travis, 1974: Light scattering in planetary atmospheres. *Space Sci. Rev.,* **16,** 527–610.

Kaufman, Y. J., and B. N. Holben, 1993: Calibration of the AVHRR visible and near-IR bands by atmospheric scattering, ocean glint and desert reflection. *Int. J. Remote Sens.,* **14,** 21–52.

King, M. D., 1987: Determination of the scaled optical thickness of clouds from reflected solar radiation measurements. *J. Atmos. Sci.,* **44,** 1734–1751.

——, and Harshvardhan, 1986: Comparative accuracy of selected multiple scattering approximations. *J. Atmos. Sci.,* **43,** 784–800.

Klein, S. A., and D. L. Hartmann, 1993: Spurious changes in the ISCCP dataset. *Geophys. Res. Lett.,* **20,** 455–458.

Kneizys, F. X., E. P. Shettle, L. W. Abreu, J. H. Chetwynd Jr., G. P. Anderson, W. O. Gallery, J. E. A. Selby, and S. A. Clough, 1988: *User's Guide to LOWTRAN 7.* AFGL-TR-88-0177, Air Force Geophysics Laboratory.

Kobayashi, T., 1993: Effects due to cloud geometry on biases in the albedo derived from radiance measurements. *J. Climate,* **6,** 120–128.

Minnis, P., P. W. Heck, D. F. Young, C. W. Fairall, and J. B. Snider, 1992: Stratocumulus cloud properties derived from simultaneous satellite- and island-based measurements during FIRE. *J. Appl. Meteor.,* **31,** 317–339.

Nakajima, T., and M. D. King, 1990: Determination of the optical thickness and effective particle radius of clouds from reflected solar radiation measurements. Part I. Theory. *J. Atmos. Sci.,* **47,** 1878–1893.

Paltridge, G. W., and C. M. R. Platt, 1976: *Radiative Processes in Meteorology and Climatology.* Elsevier Scientific, 318 pp.

Platnick, S., and S. Twomey, 1994: Determining the susceptibility of cloud albedo to changes in droplet concentrations with the Advanced Very High Resolution Radiometer. *J. Appl. Meteor.,* **33,** 334–347.

Press, W. H., B. P. Flannery, S. A. Teukolsky, and W. T. Vetterling, 1986: *Numerical Recipes: The Art of Scientific Computing,* first ed., Cambridge University Press, 818 pp.

Rossow, W. B., and R. A. Schiffer, 1991: ISCCP cloud data products. *Bull. Amer. Meteor. Soc.,* **72,** 2–20.

——, E. Kinsella, and L. C. Garder, 1983: Seasonal and global cloud variations deduced from polar orbiting satellite radiance measurements. *Proc. Fifth Conf. on Atmospheric Radiation,* Baltimore, MD, Amer. Meteor. Soc., 195–198.

——, L. C. Garder, and A. A. Lacis, 1989: Global, seasonal cloud variations from satellite radiance measurements. Part I. Sensitivity of analysis. *J. Climate,* **2,** 419–458.

——, Y. Desormeaux, C. L. Brest, and A. W. Walker, 1992: International Satellite Cloud Climatology Project (ISCCP) Radiance Calibration Report. WMO/TD No. 520, World Climate Research Program, Geneva.

Saunders, R. W., and D. P. Edwards, 1989: Atmospheric transmittances for the AVHRR channels. *Appl. Opt.,* **28,** 4154–4160.

Stamnes, K., S.-C. Tsay, W. J. Wiscombe, and K. Jayaweera, 1988: A numerically stable algorithm for discrete-ordinate-method radiative transfer in multiple scattering and emitting layers. *Appl. Opt.,* **27,** 2502–2512.

Tsay, S.-C., K. Stamnes, and K. Jayaweera, 1989: Radiative energy budget in the cloudy and hazy Arctic. *J. Atmos. Sci.,* **46,** 1002–1018.

Whitlock, C. H., W. F. Staylor, G. Smith, R. Levin, R. Frouin, C. Gautier, P. M. Teillet, P. N. Slater, Y. J. Kaufmann, B. N. Holben, W. B. Rossow, C. L. Brest, and S. R. LeCroy, 1990: AVHRR and VISSR satellite instrument calibration results for both cirrus and marine stratocumulus IFO periods. FIRE Science Report CP-3083, NASA,

Wiscombe, W. J., 1979: Mie scattering calculations—advances in technique and fast vector speed computer codes. NCAR Tech. Note TN-140+Str, National Center for Atmospheric Research, Boulder, CO.

——, 1980: Improved Mie scattering algorithms. *Appl. Opt.,* **19,** 1505–1509.